Supplementary Information

Flexible Functional Module Regulate Ultraviolet Optical Nonlinearity Achieving a Balance between Second-Harmonic Generation Response and Birefringence

Liling Cao, Haotian Tian, Donghong Lin, Chensheng Lin, Feng Xu, Yinglei Han, Tao Yan, Jindong Chen, Bingxuan Li, Ning Ye, Min Luo*

[a]College of Chemistry and Materials Science, Sichuan Normal University, Chengdu, 610068, P. R. China.

[b]Key Laboratory of Optoelectronic Materials Chemistry and Physics, Fujian Institute of Research on the Structure of Matter, Chinese Academy of Sciences, Fuzhou, Fujian 350002, China.

[c]Tianjin Key Laboratory of Functional Crystal Materials, Institute of Functional Crystal, Tianjin University of Technology, Tianjin 300384, China

[d]Fujian Science & Technology Innovation Laboratory for Optoelectronic Information of China, Fuzhou, Fujian 350002, China.

Table S1. Crystal data and structure refinement for $KLi(C_3H_2O_4)\cdot H_2O$.

Formula	$KLi(C_3H_2O_4)\cdot H_2O$
Formula weight	166.10
Crystal System	orthorhombic
Space Group	$Pna2_1$
a(Å)	8.5885(3)
b (Å)	7.5236(2)
c (Å)	9.3685(4)
α/°	90
β/°	90
γ/°	90
V(Å^3)	605.36(4)
Z	4
ρ(calcd)(g/cm^3)	1.823
Temp(K)	293(2)
λ(Å)	0.71073
F(000)	336.0
μ(mm^{-1})	0.827
R/wR($F_o^2 > 2\sigma(F_o^2)$)	0.0243/0.0652
R/wR(all data)	0.0244/0.0654
GOF on F^2	1.062
Flack parameter	0.008(15)

$R(F) = \Sigma||F_o| - |F_c||/\Sigma|F_o|$. $wR(F_o^2) = [\Sigma w(F_o^2 - F_c^2)^2/\Sigma w(F_o^2)^2]^{1/2}$

Table S2. Atomic coordinates and equivalent isotropic displacement parameters (Å^2) for $KLi(C_3H_2O_4)\cdot H_2O$.

atom	x	y	z	U(eq)
K1	6368.3(5)	2233.5(6)	533.7(8)	25.9(2)
Li1	4182(5)	5534(5)	-1156(4)	25.6(8)
C1	3029(2)	-769(3)	1799(2)	21.2(5)
C2	8698(2)	-977(3)	1874(3)	17.9(5)
C3	2422(3)	-2653(3)	1553(3)	22.5(5)
O1	3703(2)	-2(3)	789(2)	32.2(5)
O2	2828(2)	-79(2)	3010(2)	29.1(4)
O3	5529(2)	1925(2)	3434(2)	30.3(4)
O4	9128.0(19)	23(2)	872.8(18)	26.1(4)
O5	5783(2)	4048(2)	-1889(2)	28.3(4)

Table S3. Selected atomic distances (Å) for $KLi(C_3H_2O_4)\cdot H_2O$.

K1-O1^{1}	2.8998(19)	O1-C1	1.251(3)
K1-O1	2.8499(18)	C2-O4	1.258(3)
K1-O3	2.824(2)	C2-O5^{4}	1.243(3)
K1-O4^{2}	2.8384(16)	C2-C3^{5}	1.534(3)
K1-O4	2.9119(17)	O3-Li1^{6}	1.965(4)
K1-O5	2.697(2)	O4-Li1^{1}	1.948(5)
K1-O2^{1}	3.398(2)	O5-Li1	1.901(4)
K1-O2^{3}	2.949(2)	O2-C1	1.261(3)
C1-C3	1.527(3)	O2-Li1^{7}	1.950(5)

Symmetry transformations used to generate equivalent atoms:
^{1}1/2+X, 1/2-Y, +Z; ^{2}-1/2+X, 1/2-Y, +Z; ^{3}1-X, -Y, -1/2+Z; ^{4}3/2-X, -1/2+Y, 1/2+Z;
^{5}1/2+X, -1/2-Y, +Z; ^{6}1-X, 1-Y, 1/2+Z; ^{7}1/2-X, -1/2+Y, 1/2+Z

Table S4. Selected bond angles (^{o}) for $KLi(C_3H_2O_4)\cdot H_2O$.

O1-K1-O1^{1}	166.34(7)	K1-O1-K1^{3}	97.19(6)
O1^{1}-K1-O4	80.67(5)	C1-O1-K1	135.01(15)
O1-K1-O4	107.94(6)	C1-O1-K1^{3}	94.21(13)
O1^{1}-K1-O2^{1}	40.23(5)	O4-C2-C3^{4}	117.7(2)
O1-K1-O2^{2}	86.07(5)	O5^{5}-C2-O4	125.6(2)
O1^{1}-K1-O2^{2}	107.37(5)	O5^{5}-C2-C3^{4}	116.7(2)
O1-K1-O2^{1}	127.62(5)	Li1^{6}-O3-K1	94.37(13)
O3-K1-O1^{1}	98.98(6)	K1^{1}-O4-K1	97.17(5)
O3-K1-O1	70.46(6)	C2-O4-K1^{1}	135.81(15)
O3-K1-C2	74.59(6)	C2-O4-K1	100.59(13)
O3-K1-O4	93.20(6)	C2-O4-Li1^{1}	127.3(2)
O3-K1-O4^{3}	77.21(5)	Li1^{1}-O4-K1^{1}	91.77(13)
O3-K1-O2^{2}	141.96(5)	Li1^{1}-O4-K1	92.02(14)
O3-K1-O2^{1}	59.17(5)	C2^{7}-O5-K1	135.38(15)
O4^{3}-K1-O1^{1}	86.44(5)	C2^{7}-O5-Li1	127.3(2)
O4^{3}-K1-O1	82.80(5)	Li1-O5-K1	97.32(14)
O4^{3}-K1-O4	162.58(6)	K1^{8}-O2-K1^{3}	168.69(6)
O4^{3}-K1-O2^{2}	130.35(5)	C1-O2-K1^{8}	117.74(14)
O4-K1-O2^{2}	65.40(5)	C1-O2-K1^{3}	72.13(13)
O4^{3}-K1-O2^{1}	73.50(5)	C1-O2-Li1^{9}	125.4(2)
O4-K1-O2^{1}	89.11(5)	Li1^{9}-O2-K1^{8}	90.88(14)
O5-K1-O1	102.67(6)	Li1^{9}-O2-K1^{3}	78.38(14)
O5-K1-O1^{1}	80.52(6)	O4^{3}-Li1-O3^{10}	113.8(2)
O5-K1-O3	143.65(6)	O4^{3}-Li1-O2^{11}	108.6(2)
O5-K1-O4^{3}	66.46(5)	O5-Li1-O3^{1}0	114.2(2)
O5-K1-O4	122.16(5)	O5-Li1-O4^{3}	104.1(2)
O5-K1-O2^{2}	69.24(5)	O5-Li1-O2^{11}	110.9(2)

O5-K1-O2[1]	109.03(5)	O2[11]-Li1-O3[10]	105.3(2)
O2[2]-K1-O2[1]	143.89(2)	C1-C3-C2[12]	110.45(18)
O1-C1-O2	123.8(2)	O1-C1-C3	118.1(2)

Symmetry transformations used to generate equivalent atoms:
[1]1/2+X,1/2-Y,+Z; [2]1-X,-Y,-1/2+Z; [3]-1/2+X,1/2-Y,+Z; [4]1/2+X,-1/2-Y,+Z; [5]3/2-X,-1/2+Y,1/2+Z; [6]1-X,1-Y,1/2+Z; [7]3/2-X,1/2+Y,-1/2+Z; [8]1-X,-Y,1/2+Z; [9]1/2-X,-1/2+Y,1/2+Z; [10]1-X,1-Y,-1/2+Z; [11]1/2-X,1/2+Y,-1/2+Z; [12]-1/2+X,-1/2-Y,+Z

Table S5. Experimental and calculated refractive indices for KLMW. The refractive indices of KLMW were measured using prism coupling method at five different monochromatic source (407, 514, 636, 965, and 1547 nm). It follows that KLMW is a positive biaxial optical with the inequality n_z-n_y>n_y-n_x.

Wavelength (nm)	nx		ny		nz		Δn
	Exp.	Fitted.	Exp.	Fitted.	Exp.	Fitted.	
407	1.46654	1.46641	1.51816	1.51798	1.58101	1.58081	0.1145
514	1.45763	1.45763	1.50648	1.50648	1.56690	1.56690	0.1093
636	1.45272	1.45276	1.50097	1.50097	1.55992	1.55992	0.1072
965	1.44690	1.44463	1.49152	1.49118	1.54712	1.54716	0.1002
1547	1.44093	1.44092	1.48559	1.48558	1.53983	1.53982	0.0989

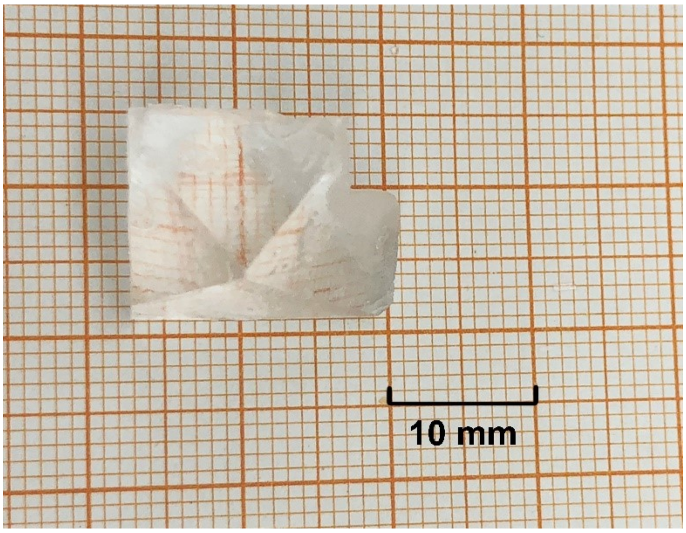

Figure S1. Centimeter-level single crystal of $KLi(C_3H_2O_4)\cdot H_2O$. The crystal quality can be further improved and the optimization is now underway.

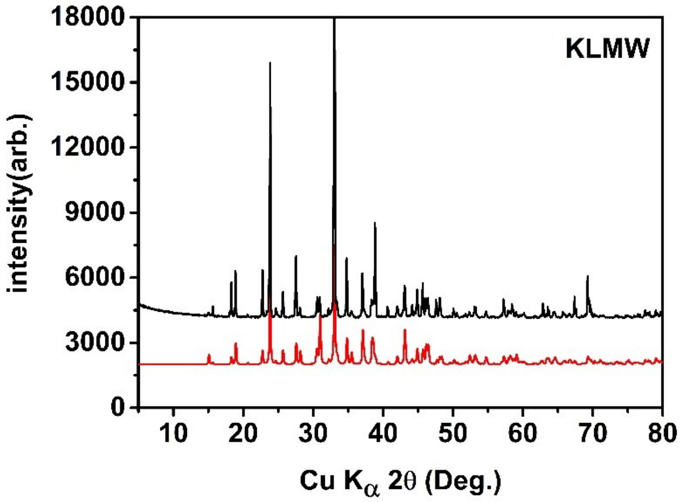

Figure S2. Experimental and calculated XRD pattern for $KLi(C_3H_2O_4)\cdot H_2O$. The red curves are the calculated ones, the black are patterns of samples.

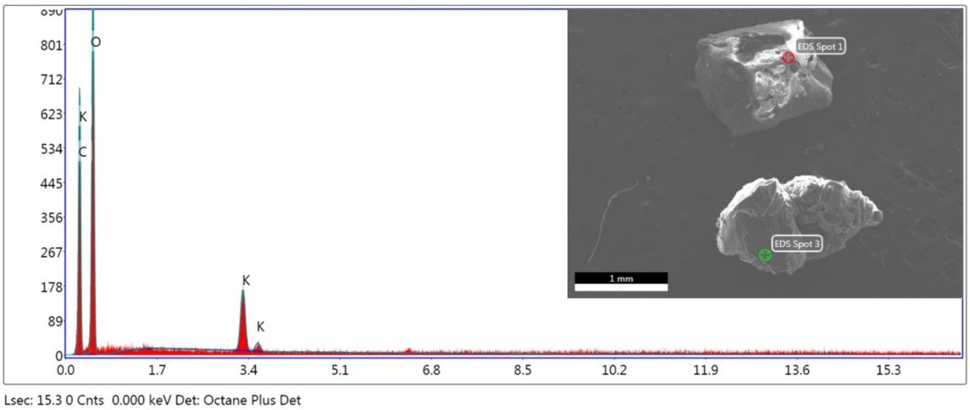

Figure S3. EDS analysis for $KLi(C_3H_2O_4){\cdot}H_2O$. The inset is the SEM image of the tested crystal.

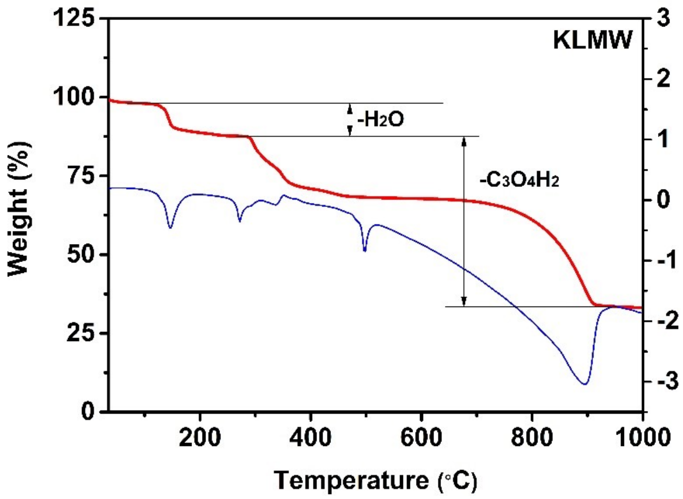

Figure S4. The TG and DTA curves of $KLi(C_3H_2O_4){\cdot}H_2O$.

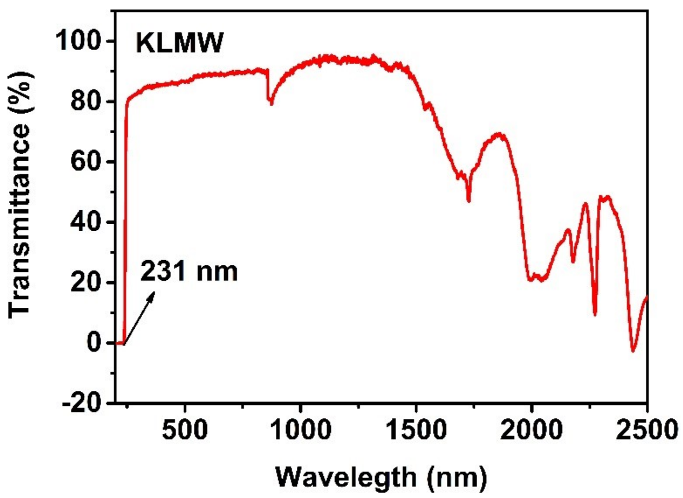

Figure S5. Ultraviolet−visible−near-infrared transmittance spectrum from 200 to 2500 nm of KLMW crystal wafer.

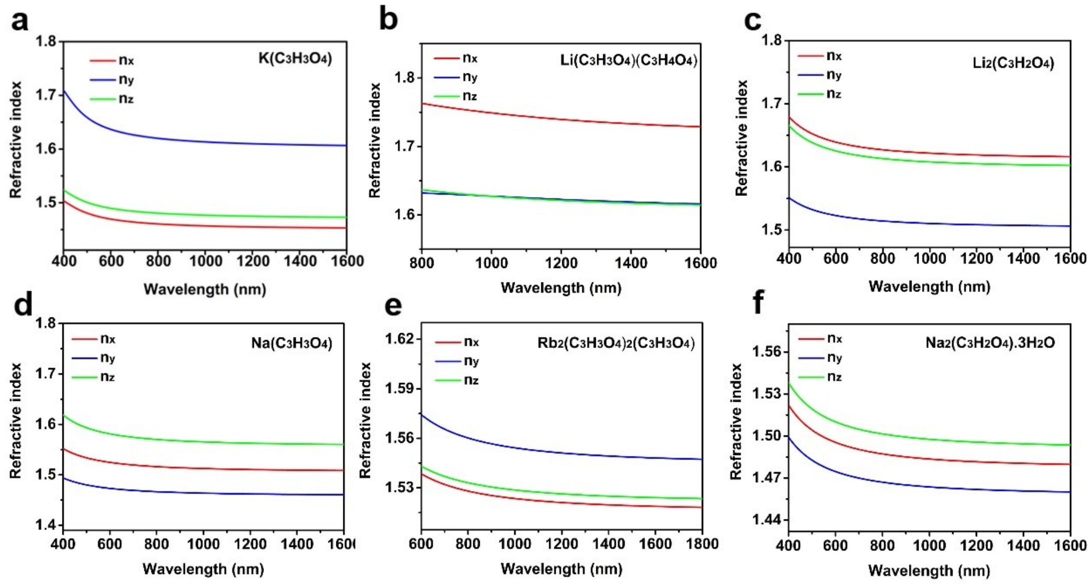

Figure S6. Calculated refractive index for **a** $K(C_3H_3O_4)$, **b** $Li(C_3H_3O_4)(C_3H_4O_4)$, **c** $Li_2(C_3H_2O_4)$, **d** $Na(C_3H_3O_4)$, **e** $Rb_2(C_3H_3O_4)_2(C_3H_4O_4)$, **f** $Na_2(C_3H_2O_4).3H_2O$.

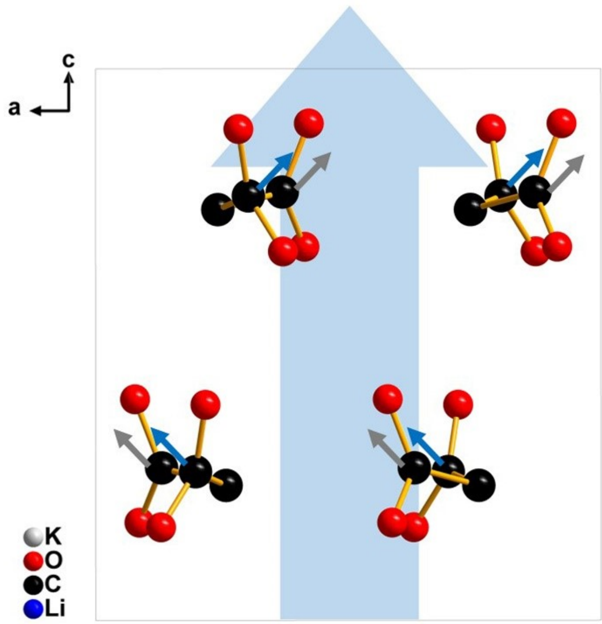

Figure S7. Polarization directions of the C(2)-centered planes (dark-gray arrows) and C(3)-centered planes (navy-blue arrows) groups and net macroscopic polarization pointing to the trans c axis (light-blue arrow).

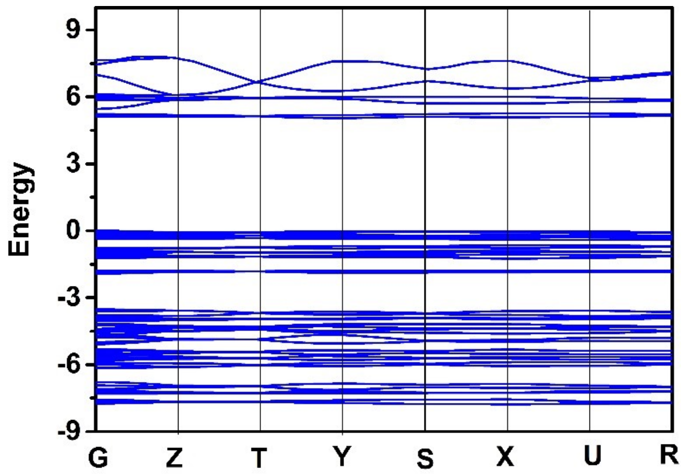

Figure S8. Band structure for $KLi(C_3H_2O_4)\cdot H_2O$.

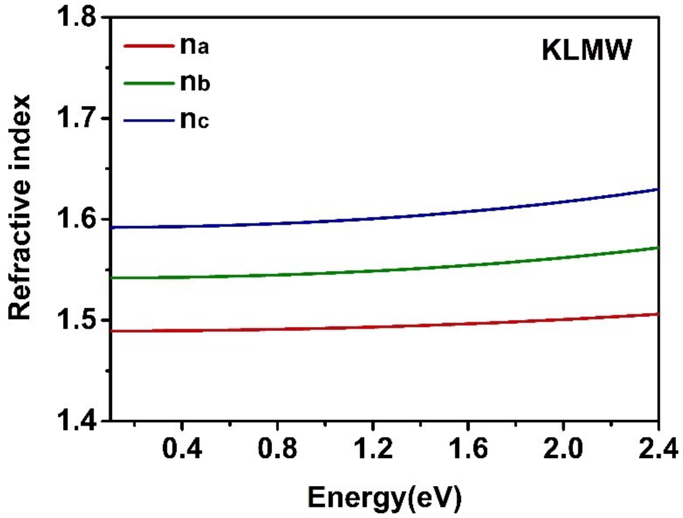

Figure S9. Calculated refractive index for $KLi(C_3H_2O_4)\cdot H_2O$.

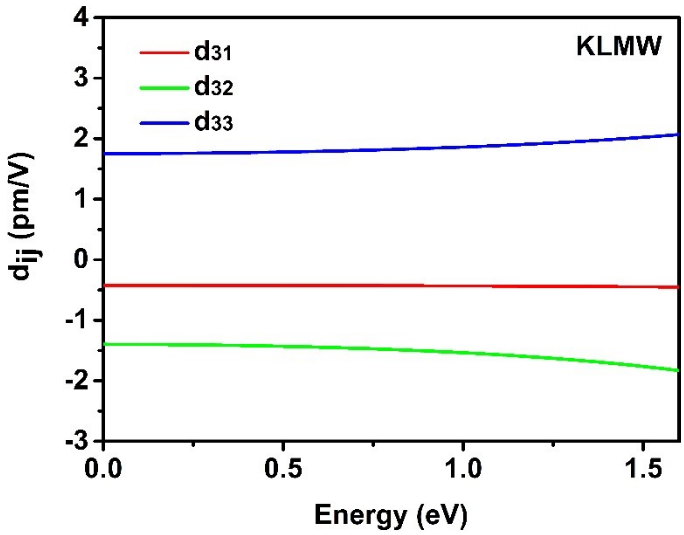

Figure S10. Calculated frequency-dependent second harmonic generation coefficients of $KLi(C_3H_2O_4)\cdot H_2O$.